Journal of Chromatography A 1674 (2022) 463120

Contents lists available at ScienceDirect

Journal of Chromatography A

journal homepage: www.elsevier.com/locate/chroma

Metal-organic framework modified carbon cloth for electric field enhanced thin film microextraction of sulfonamides in animal-derived food

Ji-Cheng Sun, Yue-Hong Pang, Cheng Yang, Xiao-Fang Shen*

State Key Laboratory of Food Science and Technology, School of Food Science and Technology, Jiangnan University, Wuxi, 214122, China

ARTICLE INFO

Article history:
Received 1 March 2022
Revised 16 April 2022
Accepted 4 May 2022
Available online 6 May 2022

Keywords:
Sulfonamides
Metal-organic framework
Electric field enhanced
Thin film microextraction
High-performance liquid chromatography

ABSTRACT

Sulfonamides (SAs) were widespread in animal-derived food at trace level, which could trigger hazards to human health. Herein, electric field enhanced thin-film microextraction (EE-TFME) was developed based on carbon cloth (CC) modified with metal-organic frameworks (MOFs) for extraction of SAs (sulfadiazine, sulfathiazole, sulfamerazine, sulfadimidine, sulfamethoxazole and sulfisoxazole), which were a series of polar analytes. MIL-101(Cr) was *in situ* synthesized on CC via hydrothermal reaction and then was used as positive electrode in EE-TFME for adsorption of SAs. Compared with traditional TFME, EE-TFME shortened extraction equilibrium time from 30 min to 15 min. Coupled with high-performance liquid chromatography (HPLC), the limits of detection (LODs) were 2.5–4.5 μg/L, while the repeatability and intermediate precision was lower than 9.1%. Quantitative determination of SAs in extracts of animal-derived samples, such as honey, pork, chicken and milk, was achieved with recoveries from 81.7% to 114.2%. The developed MOF/CC-based EE-TFME has a great potential in rapid extraction of similar polar or ionic analytes from complex food matrices.

1. Introduction

Sulfonamides (SAs), the synthetic antibiotics with p-aminobenzene structure, have been widely used to suppress bacterial growth in clinical, animal feed additives and other industries for its low production cost and broad-spectrum antibacterial activity [1]. On account of the universal use of SAs, incidents of residues (20%) detected in animal-derived food are higher frequencies than other antibiotics like tetracyclines (8%) and oxazolidinones (8%) [2]. However, the abuse of SAs can cause adverse effects to human health, such as allergic reactions, carcinogenic, teratogenic and mutagenic effects [3,4]. Thus, many countries and territories have formulated the maximum residue limit (MRL) of SAs in animal-derived food, aiming to enhance the safety of the whole food chain. Codex Alimentarius Commission (CAC), European Union (EU) and China all stipulated that the MRL of total SAs was 100 μg/kg. The MRL of sulfamethazine in fat, liver and kidney was 100 μg/kg in the United States by Food and Drug Administration (FDA), China stipulated that the MRL of sulfamethazine in milk was 25 μg/kg [4,5]. Therefore, a rapid, available and effective assay for extracting and quantifying trace levels of SAs in complex food matrix is desperately needed.

Approaches for detecting SAs abound, including high performance liquid chromatography (HPLC), electrochemical sensor assay, and immunochromatographic strip [6–8]. Among them, HPLC is a reliable method for the detection of various SAs as its high reproducibility and efficiency [9]. Effective sample pretreatment before HPLC analysis is necessary to extract, enrich and concentrate SAs from complex matrix. Recent years have seen several pretreatment methods for SAs in food samples, including solid-phase microextraction (SPME), magnetic dispersive solid–phase extraction (MSPE) and liquid-liquid extraction (LLE) [10–12]. Furthermore, thin film microextraction (TFME) which derived from SPME has gradually gained broad attention [13].

TFME has a larger volume of extractive phase with a larger surface area than SPME, which can improve sensitivity without surrendering the sampling time. In contrast to MSPE and LLE, TFME can extract the adsorbent directly from the extraction phase and consume less organic solvent. Therefore, it has been successfully applied to the pretreatment of food and biological samples [13–15]. The essential point of thin film extraction efficiency lies in coating materials, excellent materials can get favorable extraction effect,

* Corresponding author.
E-mail address: xfshen@jiangnan.edu.cn (X.-F. Shen).

https://doi.org/10.1016/j.chroma.2022.463120
0021-9673/

such as metal-organic frameworks (MOFs). MOFs, a class of hybrid materials with crystalline architectures, highly tunable porosities and different functionalities, have been heralded as promising materials for food samples preparation [16–20]. Dai et al. [21] used MIL-101(Cr) as solid phase extraction sorbents for extracting SAs, which implies that MIL-101(Cr) can be potentially used as TFME coating for extracting SAs.

The extraction equilibrium of thin film coated with MOFs relies largely on passive diffusion of analytes between the sample matrix and coating, which may lead to time-consuming process for polar or ionic compounds such as protonated amines [13]. To address this puzzle, electric field-assisted technique has been gradually adopted for improving extraction efficiency as it can result in the migration of charged targets, such as bisphenol and amphetamines [22–25]. Our group [26] also applied electrical field on SPME stainless steel fiber, which shortened the time for adsorbing bisphenol A. Despite MOFs usually exhibit very low electrical conductivity, coupling MOFs with conductive material can improve their conductivity [27]. Therefore, electrical field is potentially useful for enhancing TFME of SAs with high conductivity thin film. Carbon cloth (CC), as a commercial self-supporting substrate, is well-known for its conductivity, macropore, strong stability (high temperature resistance and strong acid resistance) and excellent flexibility, which pave the way of CC modified with MOFs towards a broad range of applications such as electrochemical detection, electrocatalysis and supercapacitors [28–30].

Considering that SAs with two amino groups tend to deprotonate, we took them as examples for similar ionic analytes. Herein, MIL-101(Cr) modified CC was applicated in electric field enhanced TFME (EE-TFME) of SAs. MIL-101(Cr) was *in situ* growth on CC surface via hydrothermal reaction for improving the conductivity, which was further used as a working electrode for the enhanced extraction of sulfadiazine, sulfathiazole, sulfamerazine, sulfadimidine, sulfamethoxazole and sulfisoxazole. SAs have similar physical properties and chemical structure with several conjugated systems, as well as the six SAs are often used in actual production, we took six SAs as typical targets. The EE-TFME combined with HPLC could successfully extract and determine SAs in animal-derived food (milk, honey, pork and chicken).

2. Experimental section

2.1. Chemicals

Carbon cloth was obtained from Taiwan Province Carbon Energy Company (Taiwan Province, China). HPLC-grade acetonitrile and methanol were bought from Fisher Chemical (Shanghai, China), chromium nitrate ($Cr(NO_3)_3{\cdot}9H_2O$) was purchased from Shanghai Macklin Biochemical Co., Ltd. (Shanghai, China), and terephthalic acid (H_2BDC) was purchased from from Shanghai Aladdin Bio-Chem Technology Co., Ltd. (Shanghai, China), hydrofluoric acid (HF, 40%), N, N-Dimethylformamide (DMF), dichloromethane, acetone, ammonia, potassium bromide, acetic acid, formic acid, acetone, ethanol, nitric acid (65%), disodium hydrogen phosphate (Na_2HPO_4), sodium dihydrogen phosphate (NaH_2PO_4) were bought from Sinopharm Chemical Reagent Co., Ltd. (Shanghai, China). Honey, milk, pork and chicken were all purchased in local supermarkets (Wuxi, China).

Sulfadiazine (SDM), sulfathiazole (ST), sulfamerazine (SMZ), sulfadimidine (SMD), sulfamethoxazole (SMX) and sulfisoxazole (SIZ) were purchased from Yuanye Biological Co., Ltd (Shanghai, China). The chemical structures of targets are shown in Table S1. Stock solutions were prepared by dissolving each substance in chromatographic grade acetonitrile at a concentration of 10 mg/mL and stored at -20°C in darkness.

2.2. Apparatus

The chromatography was performed on e2695 HPLC connected in series with 2998 photo-diode array (PDA) ultraviolet detector, then the separations were implemented on XBridge® C_{18} (4.6×250 mm, 5 μm) chromatographic column (Waters, USA). SU1510 cold field emission scanning electron microscope (SEM, Hitachi, Japan) was used to obtain SEM images. The X-ray diffraction (XRD) patterns were investigated by D2 PHASER (Bruker AXS GmbH. Karlsruhe, Germany.). Fourier-transform infrared (FT-IR) spectra were operated on IS10 FT-IR Spectrometer (Nicolet, USA). N_2 adsorption experiments were performed on Autosorb-iQ analyzer (Quantachrome, Boynton Beach, Florida, USA). Samples were vortexed on IKA vortex 3 (Germany) and centrifuged in Eppenddorf centrifuge 5810 R (Germany).

The parameters of HPLC were as follows: The loop volume was 10 μL, column temperature was 30 °C, detection wavelength was 270 nm, mobile phases were acetonitrile (A)-0.1% formic acid aqueous solution (B), gradient elution conditions was shown in Table S2. Under these conditions, the HPLC chromatogram of six SAs (SDM, ST, SMZ, SMD, SMX and SIZ) was shown in Fig. S1.

2.3. Preparation of MIL-101(Cr)/CC nanoarray

Treatment of CC. CC was washed with acetone, absolute ethyl alcohol and deionized water for 3 times, each time for 15 min at room temperature, and then dried at 60 °C for 12 h. Next, CC was soaked in concentrated nitric acid for 24 h, and then cleaned with deionized water for 3 times, and dried at 60 °C for 12 h.

CC modified with MIL-101(Cr). Firstly, 800 mg $Cr(NO_3)_3{\cdot}9H_2O$, 332 mg H_2BDC and 0.1 mL HF were uniformly dissolved in 9.6 mL deionized water at room temperature with the assistance of ultrasound. Then, the above solution and CC (1×2 cm^2) were poured into a stainless steel autoclave lined with Teflon, keeping at 220 °C for 8 h. After naturally cooling to room temperature, the obtained MIL-101(Cr)/CC material was cleaned with DMF and ethanol thoroughly [31].

2.4. Validation of the EE-TFME-HPLC-PDA method

The proposed method validation was evaluated by linearity, limits of detection (LODs), limits of quantification (LOQs), precision and trueness. Linearity for SAs was constructed with at least five levels injecting quantities between 10.0–200.0 μg/L with five replicates. The correlation coefficients (R^2) are all more than 0.9900. The LODs and LOQs were determined based on 3 and 10 times the signal-to-noise ratio (S/N), respectively. Two concentrations (50 μg/L and 100 μg/L) of the working standard solution were added to the sample and each sample was determined three times in parallel. Recoveries expressed the trueness. The precision study was determined the relative standard deviations (RSDs), which were checked through repeatability (six times a day) and intermediate (three continuous days), respectively. The matrix effect (ME) of the proposed method was calculated by the following equation: $ME{=}(A_{spiked}\text{-}A_{non}) \times 100\%/A_{pure}$, where A_{spiked} was peak area of samples spiked with SAs, A_{non} was samples spiked without SAs and A_{pure} was pure water spiked with SAs [15]. Under the optimized conditions of experiment, the matrix-matched calibration curves of samples for each SAs were constructed by plotting the peak areas and concentrations of six SAs in the range of 15.0–200.0 μg/kg, with three replicates. The recoveries of real samples spiked with SAs were calculated by the calibration curves.

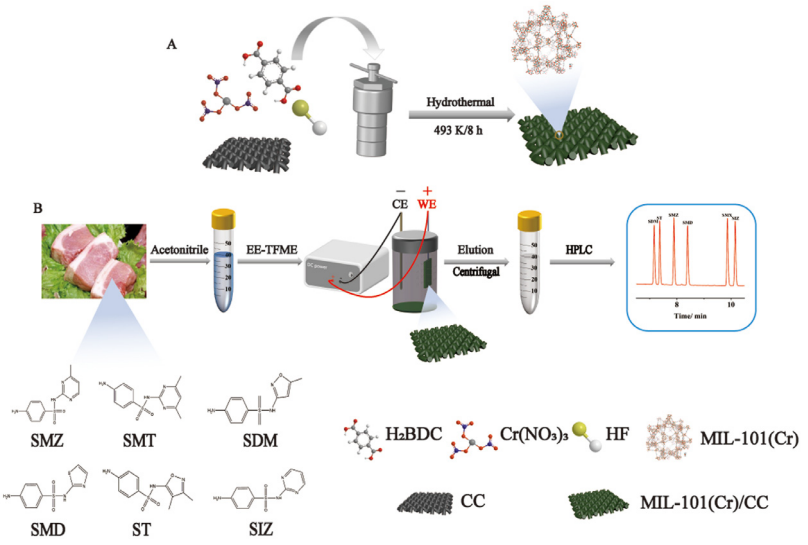

Fig. 1. The scheme for (A) the synthesis of MIL-101(Cr)/CC electrode and (B) enrichment of SAs by EE-TFME.

2.5. Real samples treatments

Pork and chicken samples were homogenized and stored at -20 °C. 8 g sample was mixed with 20 mL of 6% acetate acetonitrile solution and 5 g Na_2SO_4, centrifuged at 12628 ×g for 10 min at 4 °C after vortex for 5 min. Honey and milk samples were stored at 4 °C. 8 g honey sample was mixed with 16 mL of Na_2EDTA-McIlvaine buffer solution in centrifuge tube [32]. 8 g milk sample was mixed with 10 mL acetonitrile in centrifuge tube. Milk samples were centrifuged at 12628 ×g for 10 min at 4 °C after vortex for 1 min. The supernatant was diluted with 25 mL 0.01mol/L phosphate buffer (PB) solution (pH 4.0). 0.5 V voltage was applied on MIL-101(Cr)/CC for 15 min. Then MIL-101(Cr)/CC was eluted with 4 mL of 5% ammonia methanol solution (v/v) for 15 min, the supernatant was dried under N_2. Finally, the sample volume was fixed with 1 mL acetonitrile for HPLC analysis.

3. Results and discussions

3.1. MIL-101(Cr) modified CC for EE-TFME of SAs

Abounding π system, large windows (12 Å and 16 Å × 14.7 Å) and mesoporous pores (29 and 34 Å) that marks MIL-101(Cr) [33], it can adsorb SAs (the molecular size below 12.6 Å, Fig. S2) in the central cavity via porosity effect. After cleaning and soaking CC, MIL-101(Cr) was *in situ* synthesized on CC via a facile one-step hydrothermal method (Fig. 1A). Then we applied MIL-101(Cr)/CC for EE-TFME of typical antibiotics SAs in animal-derived food. Inserting the MIL-101(Cr)/CC electrode and platinum wire counter electrode into the solution to form a full circuit. As a positive voltage was applied to MIL-101(Cr)/CC, the negatively charged SAs formed by ionization would enrich under the action of electric field (Fig. 1B). SAs were extracted from liquid phase to MIL-101(Cr)/CC due to effect of π-π, hydrogen bonding and charge-complementary. After extracting, MIL-101(Cr)/CC was removed from the vial into 5% ammonia methanol for elution. Eventually, samples would be used for HPLC-PDA analysis and the peak area obtained was used as the analysis signal.

3.2. Characterization of MIL-101(Cr)/CC

The photograph of CC showed that it was black (Fig. 2A). When CC was modified with MIL-101(Cr), the green color of MIL-101(Cr)

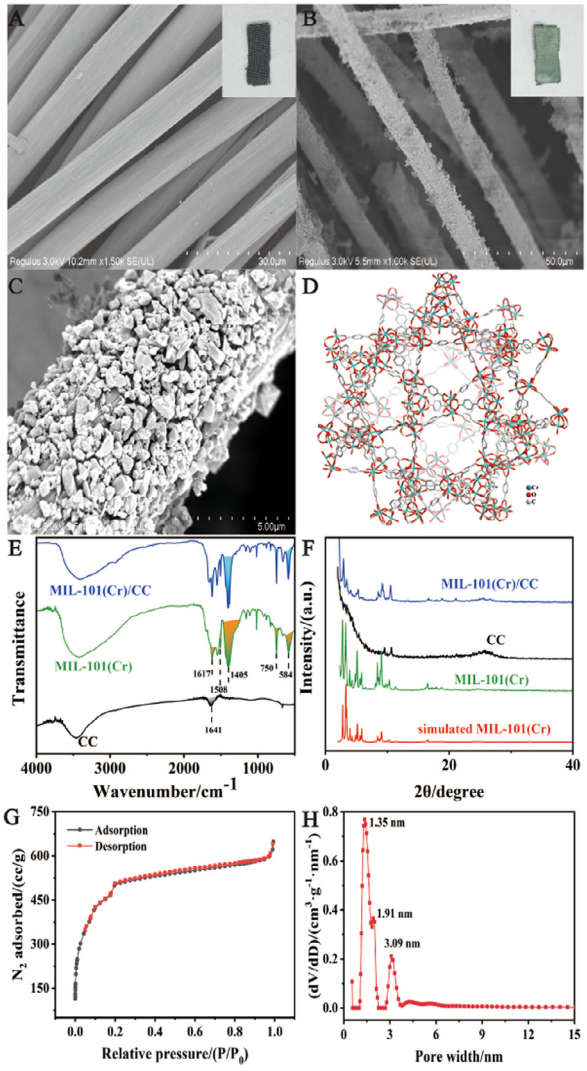

Fig. 2. (A) SEM and photograph (insert) of the bare CC. (B) SEM of MIL-101(Cr)/CC and photograph (insert) of the MIL-101(Cr)/CC. (C) SEM of MIL-101(Cr)/CC at magnifications ×10 k. (D) Structure of MIL-101(Cr) (Dimond 3.2) (E) FT-IR spectra of the MIL-101(Cr)/CC, MIL-101(Cr) and CC. (F) XRD patterns of the MIL-101(Cr)/CC, MIL-101(Cr) and CC. (G) N_2 adsorption-desorption isotherms of MIL-101(Cr)/CC at 77 K. (H) Pore size distribution of the MIL-101(Cr)/CC.

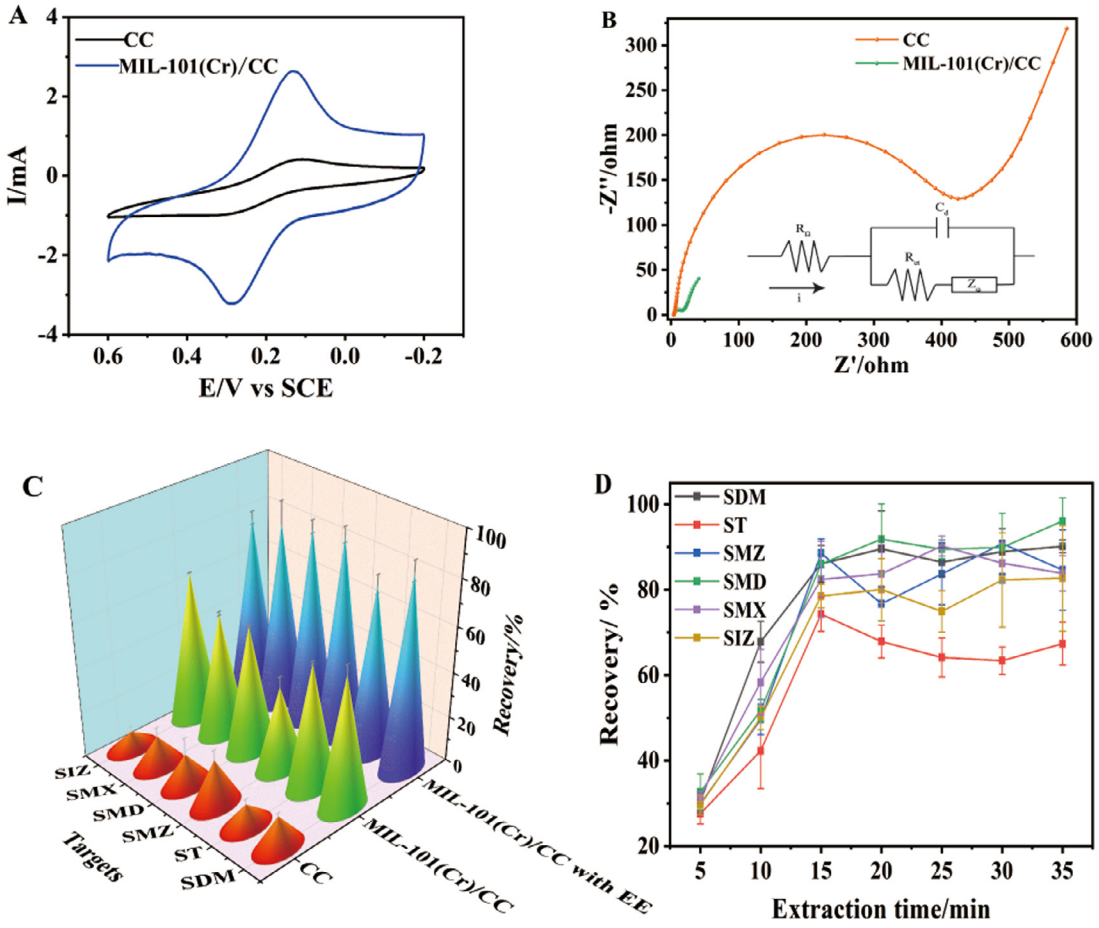

Fig. 3. (A) Cyclic voltammogram of CC and MIL-101(Cr)/CC in 5 mM $K_3[Fe(CN)_6]$ solution. (B) Nyquist plots of CC and MIL-101(Cr)/CC in 5 mM $K_3[Fe(CN)_6]$ solution and equivalent circuit model to fit the Nyquist plots (insert). (C) Comparison of recoveries of extracted SAs by CC, MIL-101(Cr)/CC and MIL-101(Cr)/CC with EE-TFME in 15 min . (pH: 7.0; extraction time: 15 min; voltage: 0.5 V; desorption solution: methanol; desorption time: 15 min). (D) Recovery of extracted SAs by MIL-101(Cr)/CC with EE-TFME ranging from 5 to 35 min (pH: 4.0; voltage: 0.5 V; desorption solution: 5% ammonia methanol solution; desorption time: 15 min).

was displayed (Fig. 2B). The morphology of CC and MIL-101(Cr)/CC were explored by SEM (Fig. 2A, B). CC is composed of carbon fibers, uniformly and densely (Fig. S3A, C). Some surface impurities were observed on the untreated carbon fiber (Fig. S3B), while the treated CC was cleaner with keeping its original morphology (Fig. S3D). The surface of the treated CC became rough, which was also conducive to the growth of MOF crystals (Fig. S4). The modified CC was still weaved with many bunches of fiber and each carbon fiber was covered with crystals (Fig. 2C). The surface of CC was uniformly modified with MIL-101(Cr) crystals that were octahedral geometry (Fig. S5). The crystals formed a super octahedral cage structure in Fd-3 m space group, and every intersection point of which was occupied by four chromium tripods bridged through six terephthalic acids (Fig. 2D).

The FT-IR spectrum displayed the high-frequency regions of MIL-101(Cr) and MIL-101(Cr)/CC were almost identical (Fig. 2E). The characteristic peaks at 584 cm^{-1} marked Cr-O group in MIL-101(Cr), and the sharp peak at 750 cm^{-1} showed that benzene had become a disubstituted product [31]. The antisymmetric and symmetric vibration peaks at around 1508 cm^{-1} and 1405 cm^{-1} demonstrated MIL-101(Cr) contained dicarboxylate group in the benzene, while the typical vibration bands from the C=C bond at 1617 cm^{-1} indicated the presence of benzene rings.

The characteristic diffraction peaks of synthesized MIL-101(Cr) appeared at 2θ = 2.75°, 3.26°, 3.92°, 5.13° and 5.84°, which was highly consistent with the simulated standard pattern (Fig. 2F). The characteristic diffraction peaks of MIL-101(Cr)/CC showed typical peaks corresponding to MIL-101(Cr) and CC (peak at 25°), which indicated that MIL-101(Cr) were successfully loaded on CC [34].

The surface area and pore structure of MIL-101(Cr)/CC were investigated by N_2 adsorption-desorption test (Fig. 2G). The prepared MIL-101(Cr)/CC gave a BET surface area of 1777 m^2/g with a pore volume of 1.50 cc/g (Fig. S6), showing a distribution of micropores and mesopores with large pore diameters (1.35 nm, 1.91 nm and 3.09 nm) (Fig. 2H), which were similar to MIL-101(Cr) in the previous report [34].

3.3. Properties of MIL-101(Cr)/CC for EE-TFME

The electrochemical properties of MIL-101(Cr)/CC were characterized by cyclic voltammogram. The oxidation-reduction potential of MIL-101(Cr)/CC and CC had little different in $K_3[Fe(CN)_6]$ solution (Fig. 3A), but the response current of MIL-101(Cr)/CC was larger, and the corresponding oxidation peak and reduction peak currents were 2.63 mA and -3.23 mA, respectively, which were 6 times and 3 times larger than CC. It may be due to the presence of open coordination metal Cr^{3+} combined with high surface area of MIL-101(Cr), which is attracted to the negatively charged $[Fe(CN)_6]^{3-}$ in the solution through electrostatic interaction, increasing the active area of the electrode and further improving the conductivity [35,36].

The electrochemical impedance of the electrode before and after modification was measured, and the equivalent circuit simulation of the electrochemical cell was carried out (Fig. 3B). The

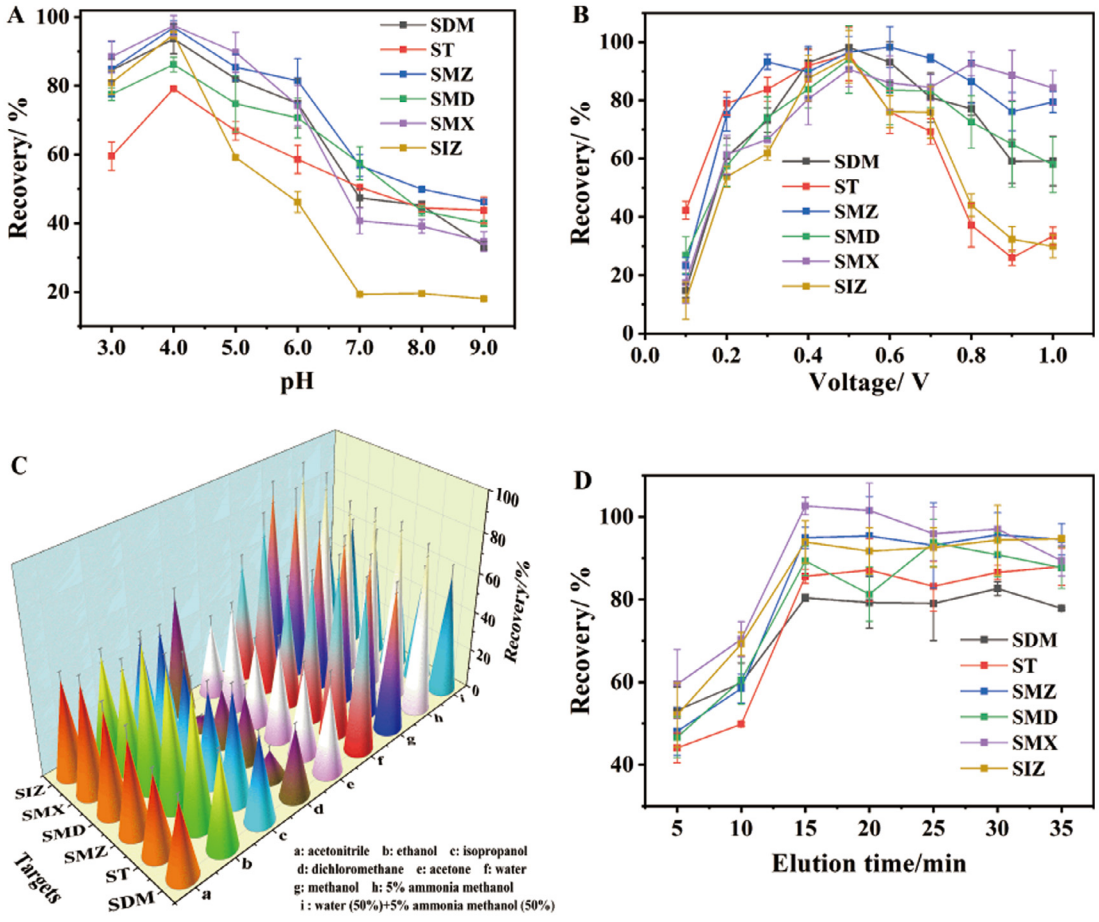

Fig. 4. (A) Recovery of extracted SAs by MIL-101(Cr)/CC diluted with PB solution pH value of 4.0–9.0. (extraction time: 15 min; voltage: 0.5 V; desorption solution: 5% ammonia methanol solution; desorption time: 15 min) (B) Recovery of extracted SAs by MIL-101(Cr)/CC with the voltage of 0.1-1.0 V (pH: 4.0; extraction time: 15 min; desorption solution: 5% ammonia methanol solution; desorption time: 15 min). (C) Recovery of extracted SAs by MIL-101(Cr)/CC eluted by acetonitrile, ethanol, isopropanol, dichloromethane, acetone, water (PB pH 9.0), methanol, 5% ammonia methanol, water (PB pH 9.0, 50%) + 5% ammonia methanol (50%) (pH: 4.0; extraction time: 15 min; voltage: 0.5 V; desorption time: 15 min). (D) Recovery of extracted SAs by MIL-101(Cr)/CC eluted with 5% ammonia methanol range from 5 to 35 min (pH: 4.0; extraction time: 15 min; voltage: 0.5 V; eluent: 5% ammonia methanol solution).

spectrum included the high-frequency and low-frequency regions of alternating current, corresponding to the charge transfer resistance (R_{ct}) and Warburg impedance (Z_{ω}) respectively. The R_{ct} (diameter of the semicircle) of CC was 452.6 Ω; while the R_{ct} of MIL-101(Cr)/CC reduced to 23.28 Ω, which proved that MIL-101(Cr)/CC had higher electron-transfer efficiency and better electrical conductivity. These advantages may result from crystals formed by the complex self-assembled of Cr^{3+} and terephthalic acid providing channels for charge transfer [31,36].

We assessed the extraction effect of modified CC with or without MIL-101(Cr) (Fig. 3C). Compared with CC, CC modified with MIL-101(Cr) gained an edge on extraction efficiency of SAs in 15 min, for instance, SIZ was 4.07 times than that of CC. To further probe whether the applied electric field would enhance extraction efficiency of MIL-101(Cr)/CC, it was used for extracting targets with the applied electric field in 15 min (Fig. 3C). The recoveries for SDM, ST, SMZ, SMD, SMX and SIZ via EE-TFME were 1.50, 1.37, 2.37, 1.53, 1.51 and 1.18 times than TFME, which indicated EE-TFME had higher extraction efficiency (Fig. S7).

Before reaching the stable equilibrium, the recoveries of SAs gradually enhanced with the increase of time in the adsorption process. Under the external voltage of 0.5 V, the equilibrium of SAs was almost about 15 min (Fig. 3D), and then the recoveries fluctuated less than 10%, among which the recoveries of SMD and SMX showed a slight downward trend that may be due to the electrochemical oxidize the three SAs to other substances [37]. Overall, the recoveries of the targets were almost unchanged after 15 min, so we chose 15 minutes as the best adsorption time. After the electric field was applied, the equilibrium of adsorption was twice faster than that without the electric field (Fig. S8), which is mainly attributed to the sulfonyl amino group deprotonated that can attract by electrostatic forces.

3.4. Optimization of EE-TFME procedure

3.4.1. Effect of pH value

The pH value is one of the essential factors affecting the extraction efficiency. Therefore, the pH value was examined from 4.0 to 9.0. The recoveries were strongest at pH 4.0 (Fig. 4A). At that condition, SAs mainly combined with MIL-101(Cr) through porosity effect, π-π effect (between benzene rings) and hydrogen bond (between -COOH and -NH_2). Along with increased pH, many electron-rich hydroxyl groups compete with SAs for adsorption on unsaturated Cr (III) sites, decreasing the extraction capacity [38]. Considering that MIL-101(Cr) would collapse under alkaline conditions [39], the extraction efficiency also reduce. Therefore, six SAs were extracted at pH 4.0.

3.4.2. Effect of voltage

SAs would be deprotonated and negatively charged in solution, which could move to MIL-101(Cr)/CC electrode by mutual attraction of positive and negative charges and electrophoresis, so the

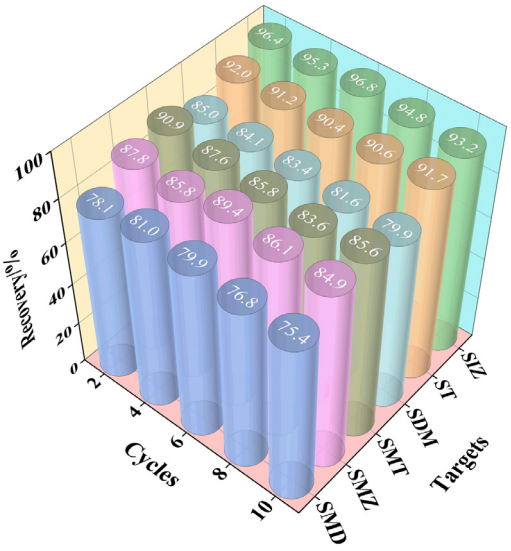

Fig. 5. Recovery of SAs with MIL-101(Cr)/CC for each extraction cycle.

positive voltage applied to MIL-101(Cr)/CC was an important parameter of EE-TFME. Voltage from 0.1 to 1.0 V was studied. The EE-TFME efficiency for SAs enhanced with the increase of voltage from 0.1 to 0.5 V (Fig. 4B). Whereas, when voltage exceeded 0.5 V, the extraction efficiency decreased gradually. On the one hand, SAs may be oxidized to other substances at higher voltage [37]. On the other hand, when the voltage increased to a certain extent, a compressed electric double layer effect formed, which would lead to the thinning of the adsorption layer and reduce the adsorption effect [40]. Therefore, the voltage of 0.5 V was selected.

3.4.3. Selection of ionic strength

Ionic strength could increase the conductivity of the solution, but it may affect the extraction efficiency. PB solution (pH 4.0) consisted of NaH_2PO_4, which was used to ensure the conductivity of the solution and provide ionic strength. Therefore, the EE-TFME efficiency was investigated by changing concentrations of NaH_2PO_4 in 25 mL PB solution from 0.12% to 20%. With the increase of ionic strength, the recoveries decreased slightly, which may be due to the increase of solution viscosity and the "invasion" effect of metal ions on MOFs channels (Fig. S9). Therefore, we carried out following experiments in 0.12% (0.01 mol/L) PB solution.

3.4.4. Selection of desorption solution

To improve the desorption between SAs and MIL-101(Cr)/CC as much as possible, the desorption solvent must have higher affinity for the targets than MIL-101(Cr)/CC. Considering the characteristics of this experiment and previous reports, several desorption solvents were tested, including acetonitrile, ethanol, isopropanol, dichloromethane, acetone, water, methanol, 5% ammonia methanol solution and the mixed solution of water (50%) spiked with 5% ammonia methanol (50%). The result of the best desorption solution was 5% ammonia methanol (Fig. 4C). Because appropriate alkaline conditions could facilitate the elution of SAs from MOF [38]. Furthermore, the open metal sites of MIL-101(Cr)/CC have greater affinity for polar solvents [41]. Moreover, the voltage between the two electrodes was reversed in the elution process with PB (pH 9.0). After the reversal, the same charge between the targets and the electrode repelled each other, which made the elution effect in water better. However, it was still weaker than 5% ammonia methanol solution. Finally, 5% ammonia methanol was used as the desorption solvent for the subsequent experiments.

3.4.5. Effect of eluent volume and elution time

The effect of eluent volume was studied from 3 to 7 mL. When the volume was 4 mL, recoveries of SAs reached the highest (Fig. S10). Otherwise, the influence of elution time was studied by changing the elution time in the range of 5–35 min (Fig. 4D). Within 5–15 min, the recoveries of most SAs gradually increased, and no significant change was observed when the extraction time was further prolonged. Therefore, 4 mL was selected as the best volume and 15 min was the best elution time.

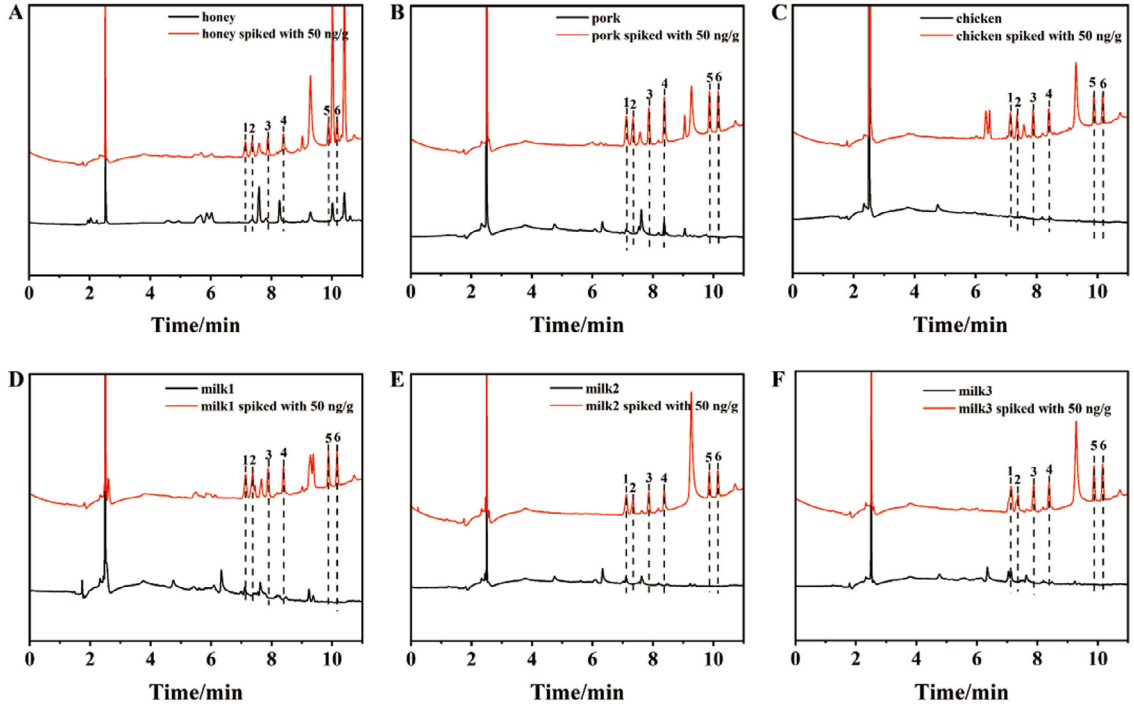

Fig. 6. HPLC chromatograms of (A) honey, (B) pork, (C) chicken (D) milk1, (E)milk2 and (F) milk3. 1-SDM, 2-ST, 3-SMZ, 4-SMD, 5-SMX, 6-SIZ.

Table 1
Analytical performance and parameters of the proposed method.

Analytes	R^2	LOD (μg/L)	LOQ (μg/L)	Linear range (μg/L)	RSD (50 μg/L, %)		ME (%)					
					repeatability (n=6)	intermediate (n=3)	honey	pork	chicken	milk1	milk2	milk3
SDM	0.9915	3.5	12.5	12.5–200.0	3.7	9.1	94.7	99.7	93.7	98.2	98.4	97.0
ST	0.9967	4.5	14.5	14.5–200.0	4.8	8.7	97.6	92.0	103.7	106.1	94.2	103.1
SMZ	0.9922	4.0	12.5	13.0–200.0	5.9	5.8	98.2	95.8	93.4	99.8	96.8	93.8
SMD	0.9965	2.8	10.0	10.5–200.0	6.3	4.7	107.9	98.7	97.4	97.6	95.3	93.6
SMX	0.9936	2.5	9.0	10.0–200.0	7.8	8.3	95.4	92.1	99.6	98.7	99.7	99.1
SIZ	0.9912	2.5	8.0	10.0–200.0	3.5	7.7	91.4	103.5	99.1	99.8	98.7	98.5

Table 2
Comparison of proposed method with other reported methods for determining SAs.

Method	Adsorbent	Extraction time/min	LOD/ (ng/mL)	LOQ/ (ng/mL)	Linear range/ (ng/mL)	Refs
SPE-spectrophotometric detection	hypercrosslinked polystyrene	30	20–50	-	70–3000	[49]
BAμE-μLD-HPLC-DAD	polystyrene-divinylbenzene polymer	960	0.08–0.16	0.26–0.53	0.16–8.0	[42]
LLE-HPLC-MS/MS	0.1% formic acid acetonitrile solution	20	2.5–10.0	5.0–25.0	5.0–1000.0	[46]
MSPD-LC-MS/MS	N-vinylpyrrolidone and lipophilic divinylbenzene	6	2.3–16.4	6.9–54.7	6.9–100	[47]
SPE-LC-MS	Sep-Pack® C_{18}	30	0.83–4.27	1.16–5.06	0–200	[43]
LLE-HPLC-DAD	Chloroform/Acetone	40	0.9–5.0	2.7–15.1	10–200	[44]
MSPE-DLLME-HPLC-DAD	MCNs/NaCl octanol solution	65	1–5	2–10	2–400	[45]
SALLE/online SPE-HPLC-UV	Acetonitrile/anion-exchange resin cartridge	-	5.0–7.5	15.0–22.5	50–3000	[48]
EE-TFME-HPLC-PDA	MIL-101(Cr)/CC	15	2.5–4.5	8.0–14.5	10.0–200.0	This work

BAμE-μLD: bar adsorption microextraction combined with microliquid desorption; LLE: liquid-liquid extraction; MSPD: matrix dispersion solid phase extraction; MSPE-DLLME: magnetic solid phase extraction combined with dispersion liquid-liquid microextraction; SALLE: salting out liquid-liquid extraction.

3.5. Analytical method validation

Under the optimized extraction conditions, the analytical properties of EE-TFME were evaluated (Table 1). The concentration range of six SAs which the calibration curve was linear in 10.0–200.0 μg/L, as well as $R^2 \geq 0.9912$. The LODs and LOQs for SAs were in the range of 2.5–4.5 μg/L and 8.0–14.5 μg/L, respectively. To ensure reusability of MIL-101(Cr)/CC, performance testing was conducted by analyzing extraction efficiency of SAs for ten cycles, the recoveries of which ranged from 76.43% to 96.40% (Fig. 5). Additionally, the RSDs of repeatability and intermediate were below 7.8% and 9.1%, respectively. To further demonstrate the stability of MIL-101(Cr)/CC, the structure and morphology of it (before and after EE-TFME) were explored (Fig. S11). The ME of six samples ranged from 91.4% to 107.9%, indicating that the efficiency of EE-TFME was not significantly affected by the sample matrix.

In contrast to the other methods (Table 2), bar adsorption microextraction combined with microliquid desorption took 960 min to reach extraction equilibrium, SPE combined with Sep-Pack® C_{18} or hypercrosslinked polystyrene both took 30 min, LLE with chloroform/acetone and MSPE with MCNs/NaCl octanol solution consumed 40 min and 65 min, EE-TFME only 15 min [42–45]. Compared with LLE with 0.1% formic acid acetonitrile solution or chloroform/acetone, EE-TFME consumed less organic solvent and shorter time with lower LODs [46]. Otherwise, EE-TFME had lower LODs and LOQs than matrix dispersion solid phase extraction with N-vinylpyrrolidone/lipophilic divinylbenzene and salting out LLE acetonitrile/anion-exchange resin cartridge [47,48].

Table 3
Concentrations(μg/kg), RSD (%, n=3) and spike recoveries (%) of SAs in real samples.

Real sample	Spiked concentration	Recovery (RSD)					
		SDM	ST	SMZ	SMD	SMX	SIZ
Honey	0	ND	<LOQ	ND	ND	ND	ND
	50	97.9 (3.5)	108.6 (4.6)	97.4 (4.6)	98.9 (6.9)	93.7 (6.8)	99.4 (7.6)
	100	91.9 (3.1)	96.4 (8.0)	94.6 (4.1)	100.7 (6.4)	86.1 (1.9)	89.9 (6.7)
Pork	0	14.7 (3.7)	ND	ND	24.4 (5.3)	ND	ND
	50	99.7 (5.6)	95.2 (2.4)	99.1 (7.3)	102.3 (5.2)	95.2 (6.3)	98.4 (3.8)
	100	98.1 (3.0)	98.5 (1.5)	98.1 (3.5)	96.9 (7.7)	91.8 (6.4)	92.2 (8.6)
Chicken	0	ND	ND	ND	ND	ND	ND
	50	114.2 (5.0)	112.2 (8.5)	94.2 (8.2)	113.3 (7.5)	97.5 (7.9)	96.8 (6.1)
	100	97.1 (4.0)	99.6 (1.8)	83.8 (3.7)	86.9 (6.4)	92.6 (7.0)	92.1 (6.8)
Milk1	0	<LOQ	ND	ND	ND	ND	ND
	50	94.9 (7.8)	94.6 (5.6)	93.0 (6.6)	91.7 (3.8)	91.6 (8.3)	84.4 (3.8)
	100	82.6 (3.7)	88.9 (5.1)	87.0 (7.1)	87.6 (8.3)	87.4 (4.4)	82.7 (6.4)
Milk2	0	ND	ND	ND	ND	ND	ND
	50	106.0 (7.8)	91.8 (5.6)	98.4 (8.2)	93.7 (6.4)	97.4 (1.7)	98.7 (2.6)
	100	92.4 (3.4)	92.7 (3.2)	96.9 (5.2)	83.3 (3.1)	94.1 (2.8)	93.0 (2.1)
Milk3	0	<LOQ	ND	ND	ND	ND	ND
	50	98.1 (5.3)	104.5 (1.7)	99.6 (3.6)	104.1 (5.5)	97.4 (1.5)	101.8 (3.7)
	100	93.4 (4.8)	84.6 (6.2)	81.7 (6.8)	92.1 (5.6)	95.0 (7.1)	92.5 (6.3)

ND: Not detected.

3.6. Analysis of real samples

The method was applied to extracting and determining SAs in six animal-derived food (honey, milk, pork and chicken) at 50 and 100 μg/kg to evaluate its practical applicability. The typical HPLC chromatograms of the blank animal-derived food samples and samples spiked with 50 μg/kg of SAs indicated a low noise and matrix interference (Fig. 6). ST was detected in honey, SDM was detected in milk and pork, while SMD was found in pork at 24.4 μg/kg (all below the MRL of EU). Recoveries for six SAs in samples ranged from 81.7% to 114.2% and RSDs ranged from 1.5% to 8.6%, which also validated the trueness of the developed method (Table 3). Recoveries of samples spiked with 50 μg/kg were higher than those of 100 μg/kg, which may result from the fact that it is difficult for the adsorbent to adsorb all SAs with the increase of spiked concentration.

4. Conclusions

In summary, we explored a rapid EE-TFME method based on MIL-101(Cr)/CC, and combined it with HPLC-PDA for determination of six SAs in animal-derived food (honey, pork, chicken and milk). The developed method facilitated movement of SAs to MIL-101(Cr)/CC with satisfactory extraction recoveries by applying an electric field to speed up extraction equilibrium. Intriguingly, as its high conductivity and mechanical flexibility, MIL-101(Cr)/CC owns a large niche market in the pretreatment and detection of other food samples. Overall, the method provides a methodological basis to the future use other types of MOFs in EE-TFME for food safety.

Declaration of Competing Interest

The authors declare that they have no known competing financial interests or personal relationships that could have appeared to influence the work reported in this paper.

CRediT authorship contribution statement

Ji-Cheng Sun: Conceptualization, Methodology, Formal analysis, Investigation, Writing – original draft. **Yue-Hong Pang:** Methodology, Formal analysis, Validation, Investigation, Funding acquisition. **Cheng Yang:** Conceptualization, Methodology, Investigation. **Xiao-Fang Shen:** Conceptualization, Resources, Writing – review & editing, Project administration, Funding acquisition.

Acknowledgments

This work was supported by the National Natural Science Foundation of China (22076067, 21976070), and the Fundamental Research Funds for the Central Universities (JUSRP22003).

Supplementary materials

Supplementary material associated with this article can be found, in the online version, at doi:10.1016/j.chroma.2022.463120.

References

[1] L. Wen, L. Liu, X. Wang, M.-L. Wang, J.-M. Lin, R.-S. Zhao, Spherical mesoporous covalent organic framework as a solid-phase extraction adsorbent for the ultrasensitive determination of sulfonamides in food and water samples by liquid chromatography-tandem mass spectrometry, J. Chromatogr. A 1625 (2020) 461275.
[2] T. Chatzimitakos, V. Samanidou, C.D. Stalikas, Graphene-functionalized melamine sponges for microextraction of sulfonamides from food and environmental samples, J. Chromatogr. A 1522 (2017) 1–8.
[3] S.J. Stohs, M.J.S. Miller, A case study involving allergic reactions to sulfur-containing compounds including, sulfite, taurine, acesulfame potassium and sulfonamides, Food Chem. Toxicol. 63 (2014) 240–243.
[4] W. Jia, A. Du, Z. Fan, L. Shi, High-coverage screening of sulfonamide metabolites in goat milk by magnetic doped S graphene combined with ultrahigh-performance liquid chromatography-high-resolution mass spectrometry, J. Agric. Food Chem. 69 (2021) 4755–4765.
[5] A.D. Corcia, M. Nazzari, Liquid chromatographic-mass spectrometric methods for analyzing antibiotic and antibacterial agents in animal food products, J. Chromatogr. A 974 (2002) 53–89.
[6] Y. Chen, L. Guo, L. Liu, S. Song, H. Kuang, C. Xu, Ultrasensitive immunochromatographic strip for fast screening of 27 sulfonamides in honey and pork liver samples based on a monoclonal antibody, J. Agric. Food Chem. 65 (2017) 8248–8255.
[7] A.N.M. Nasir, N. Yahaya, N.N.M. Zain, V. Lim, S. Kamaruzaman, B. Saad, N. Nishiyama, N. Yoshida, Y. Hirota, Thiol-functionalized magnetic carbon nanotubes for magnetic micro-solid phase extraction of sulfonamide antibiotics from milks and commercial chicken meat products, Food Chem. 276 (2019) 458–466.
[8] J. Xiao, X. Hu, K. Wang, Y. Zou, E. Gyimah, S. Yakubu, Z. Zhang, A novel signal amplification strategy based on the competitive reaction between 2D Cu-TCPP (Fe) and polyethyleneimine (PEI) in the application of an enzyme-free and ultrasensitive electrochemical immunosensor for sulfonamide detection, Biosens. Bioelectron. 150 (2020) 111883.
[9] H.J. Kim, M.H. Jeong, H.J. Park, W.C. Kim, J.E. Kim, Development of an immunoaffinity chromatography and HPLC-UV method for determination of 16 sulfonamides in feed, Food Chem. 196 (2016) 1144–1149.
[10] K.-H. Lu, C.-Y. Chen, M.-R. Lee, Trace determination of sulfonamides residues in meat with a combination of solid-phase microextraction and liquid chromatography-mass spectrometry, Talanta 72 (2007) 1082–1087.
[11] p-S. Gao, Y. Guo, X. Li, X. Wang, J. Wang, F. Qian, H. Gu, Z. Zhang, Magnetic solid phase extraction of sulfonamides based on carboxylated magnetic graphene oxide nanoparticles in environmental waters, J. Chromatogr. A 1575 (2018) 1–10.
[12] T. Yao, K. Du, Simultaneous determination of sulfonamides in milk: in-situ magnetic ionic liquid dispersive liquid-liquid microextraction coupled with HPLC, Food Chem. 331 (2020) 127342.
[13] Y.A. Olcer, M. Tascon, A.E. Eroglu, E. Boyacı, Thin film microextraction: towards faster and more sensitive microextraction, TrAC Trend. Anal. Chem. 113 (2019) 93–101.
[14] Z. Mehrani, H. Ebrahimzadeh, E. Moradi, Poly m-aminophenol/nylon 6/graphene oxide electrospun nanofiber as an efficient sorbent for thin film microextraction of phthalate esters in water and milk solutions preserved in baby bottle, J. Chromatogr. A 1600 (2019) 87–94.
[15] Z. Liu, W. Li, X. Zhu, R. Hua, X. Wu, J. Xue, Combination of polyurethane and polymethyl methacrylate thin films as a microextraction sorbent for rapid adsorption and sensitive determination of neonicotinoid insecticides in fruit juice and tea by ultra high performance liquid chromatography with tandem mass spectrometry, J. Chromatogr. A 1659 (2021) 462646.
[16] L. Lian, X. Zhang, J. Hao, J. Lv, X. Wang, B. Zhu, D. Lou, Magnetic solid-phase extraction of fluoroquinolones from water samples using titanium-based metal-organic framework functionalized magnetic microspheres, J. Chromatogr. A 1579 (2018) 1–8.
[17] Z. Zhou, Y. Fu, Q. Qin, X. Lu, X. Shi, C. Zhao, G. Xu, Synthesis of magnetic mesoporous metal-organic framework-5 for the effective enrichment of malachite green and crystal violet in fish samples, J. Chromatogr. A 1560 (2018) 19–25.
[18] P.-L. Wang, L.-H. Xie, E.A. Joseph, J.-R. Li, X.-O. Su, H.-C. Zhou, Metal-organic frameworks for food safety, Chem. Rev. 119 (2019) 10638–10690.
[19] S. Moinfar, A. Khodayari, S. Sohrabnezhad, A. Aghaei, L.A. Jamil, MIL-53 (Al)/Fe_2O_3 nanocomposite for solid-phase microextraction of organophosphorus pesticides followed by GC-MS analysis, Microchim. Acta 187 (2020) 1–10.
[20] P. Zhou, W. Zhang, X. Wang, Development of a syringe membrane-based microextraction method based on metal-organic framework mixed-matrix membranes for preconcentration/extraction of polycyclic aromatic hydrocarbons in tea infusion, Food Chem. 361 (2021) 130105.
[21] X. Dai, X. Jia, P. Zhao, T. Wang, J. Wang, P. Huang, L. He, X. Hou, A combined experimental/computational study on metal-organic framework MIL-101(Cr) as a SPE sorbent for the determination of sulphonamides in environmental water samples coupling with UPLC-MS/MS, Talanta 154 (2016) 581–588.
[22] J. Zeng, J. Zou, X. Song, J. Chen, J. Ji, B. Wang, Y. Wang, J. Ha, X. Chen, A new strategy for basic drug extraction in aqueous medium using electrochemically enhanced solid-phase microextraction, J. Chromatogr. A 1218 (2011) 191–196.
[23] J. Zhang, C. Wen, Q. Li, B.E. Meteku, R. Zhao, B. Cui, X. Li, J. Zeng, Electro-enhanced solid-phase microextraction of bisphenol A from thermal papers using a three-dimensional graphene coated fiber, J. Chromatogr. A 1585 (2019) 27–33.
[24] J. Zeng, Y. Li, X. Zheng, Z. Li, T. Zeng, W. Duan, Q. Li, X. Shang, B. Dong, Controllable transformation of aligned ZnO nanorods to ZIF-8 as solid-phase microextraction coatings with tunable porosity, polarity, and conductivity, Anal. Chem. 91 (2019) 5091–5097.
[25] R. Xu, H.K. Lee, Application of electro-enhanced solid phase microextraction combined with gas chromatography-mass spectrometry for the determination of tricyclic antidepressants in environmental water samples, J. Chromatogr. A 1350 (2014) 15–22.
[26] Y.-H. Pang, Y.-Y. Huang, X.-F. Shen, Y.-Y. Wang, Electro-enhanced solid-phase microextraction with covalent organic framework modified stainless steel fiber for efficient adsorption of bisphenol A, Anal. Chim. Acta 1142 (2021) 99–107.

[27] Z. Xu, Q. Wang, H. Zhangsun, S. Zhao, Y. Zhao, L. Wang, Carbon cloth-supported nanorod-like conductive Ni/Co bimetal MOF: a stable and high-performance enzyme-free electrochemical sensor for determination of glucose in serum and beverage, Food Chem. 349 (2021) 129202.
[28] Q. Zha, M. Li, Z. Liu, Y. Ni, Hierarchical Co, Hierarchical Co, Fe–MOF-74/Co/Carbon cloth hybrid electrode: simple construction and enhanced catalytic performance in full water splitting, ACS Sustain. Chem. Eng. 8 (2020) 12025–12035.
[29] T. Zhe, R. Li, F. Li, S. Liang, D. Shi, X. Sun, Y. Liu, Y. Cao, T. Bu, L. Wang, Surface engineering of carbon selenide nanofilms on carbon cloth: an advanced and ultrasensitive self-supporting binder-free electrode for nitrite sensing, Food Chem. 340 (2021) 127953.
[30] Z. Zhu, Z. Zhang, Q. Zhuang, F. Gao, Q. Liu, X. Zhu, M. Fu, Growth of $MnCo_2O_4$ hollow nano-spheres on activated carbon cloth for flexible asymmetric supercapacitors, J. Power Sources 492 (2021) 229669.
[31] F. Zhang, T. Niu, F. Wu, L. Wu, G. Wang, J. Li, Highly oriented MIL-101(Cr) continuous films grown on carbon cloth as efficient polysulfide barrier for lithium-sulfur batteries, Electrochim. Acta 392 (2021) 139028.
[32] Y.-H. Pang, Z.-Y. Lv, J.-C. Sun, C. Yang, X.-F. Shen, Collaborative compounding of metal-organic frameworks for dispersive solid-phase extraction HPLC-MS/MS determination of tetracyclines in honey, Food Chem. 355 (2021) 129411.
[33] X. Han, P. Liu, F. Lin, W. Chen, R. Luo, Q. Han, Z. Jiang, X. Wang, S. Song, K.M. Reddy, H. Deng, M. Chen, Structures and structural evolution of sublayer surfaces of MOF crystals, Angew. Chem. Int. Edit. 59 (2020) 21419–21424.
[34] G. Férey, C. Mellot-Draznieks, C. Serre, F. Millange, J. Dutour, S. Surblé, I. Margiolaki, A chromium terephthalate-based solid with unusually large pore volumes and surface area, Science 309 (2005) 2040–2042.
[35] A. Morozan, F. Jaouen, Metal organic frameworks for electrochemical applications, Energy Environ. Sci. 5 (2012) 9269–9290.
[36] D. Sheberla, J.C. Bachman, J.S. Elias, C.J. Sun, Y. Shao-Horn, M. Dincă, Conductive MOF electrodes for stable supercapacitors with high areal capacitance, Nat. Mater. 16 (2017) 220–224.
[37] M. Chen, L. Ren, K. Qi, Q. Li, M. Lai, Y. Li, X. Li, Z. Wang, Enhanced removal of pharmaceuticals and personal care products from real municipal wastewater using an electrochemical membrane bioreactor, Bioresource Technol. 311 (2020) 123579.
[38] X. Jia, P. Zhao, X. Ye, L. Zhang, T. Wang, Q. Chen, X. Hou, A novel metal-organic framework composite MIL-101(Cr)@GO as an efficient sorbent in dispersive micro-solid phase extraction coupling with UHPLC-MS/MS for the determination of sulfonamides in milk samples, Talanta 169 (2017) 227–238.
[39] S.-H. Huo, X.-P. Yan, Facile magnetization of metal-organic framework MIL-101 for magnetic solid-phase extraction of polycyclic aromatic hydrocarbons in environmental water samples, Analyst 137 (2012) 3445–3451.
[40] J. Chun, B.U. Ye, J.W. Lee, D. Choi, C.Y. Kang, S.W. Kim, Z.L. Wang, J.M. Baik, Boosted output performance of triboelectric nanogenerator via electric double layer effect, Nat. Commun. 7 (2016) 1–9.
[41] Y.-Y. Fu, C.-X. Yang, X.-P. Yan, Control of the coordination status of the open metal sites in metal-organic frameworks for high performance separation of polar compounds, Langmuir 28 (2012) 6794–6802.
[42] A.H. Ide, S.M. Ahmad, N.R. Neng, J.M.F. Nogueira, Enhancement for trace analysis of sulfonamide antibiotics in water matrices using bar adsorptive microextraction (BAμE), J. Pharm. Biomed. Anal. 129 (2016) 593–599.
[43] I. Guillén, L. Guardiola, L. Almela, E. Núñez-Delicado, J.A. Gabaldón, Simultaneous determination of nine sulphonamides by LC-MS for routine control of raw honey samples, Food Anal. Method. 10 (2017) 1430–1441.
[44] A. Armentano, S. Summa, S.L. Magro, C. Palermo, D. Nardiello, D. Centonze, M. Muscarella, Rapid method for the quantification of 13 sulphonamides in milk by conventional high-performance liquid chromatography with diode array ultraviolet detection using a column packed with core-shell particles, J. Chromatogr. A 1531 (2018) 46–52.
[45] N. Yazdanfar, M. Shamsipur, M. Ghambarian, Determination of sulfonamide residues in animal foodstuffs by magnetic dispersive solid-phase extraction using magnetic carbon nanocomposites coupled with ion pair-dispersive liquid–liquid micro-extraction combined with HPLC-DAD, J. Iran. Chem. Soc. 18 (2020) 1433–1442.
[46] J. Li, H. Liu, J. Zhang, Y. Liu, L. Wu, A novelty strategy for the fast analysis of sulfonamide antibiotics in fish tissue using magnetic separation with high-performance liquid chromatography-tandem mass spectrometry, Biomed. Chromatogr. 30 (2016) 1331–1337.
[47] Q. Shen, R. Jin, J. Xue, Y. Lu, Z. Dai, Analysis of trace levels of sulfonamides in fish tissue using micro-scale pipette tip-matrix solid-phase dispersion and fast liquid chromatography tandem mass spectrometry, Food Chem. 194 (2016) 508–515.
[48] K. Fikarová, B. Horstkotte, D. Machián, H. Sklenářová, P. Solich, Lab-In-Syringe for automated double-stage sample preparation by coupling salting out liquid-liquid extraction with online solid-phase extraction and liquid chromatographic separation for sulfonamide antibiotics from urine, Talanta 221 (2021) 121427.
[49] S.G. Dmitrienko, E.V. Kochuk, V.V. Tolmacheva, V.V. Apyari, Y.A. Zolotov, Determination of the total content of some sulfonamides in milk using solid-phase extraction coupled with off-line derivatization and spectrophotometric detection, Food Chem. 188 (2015) 51–56.